Parallel dynamics of extremely diluted symmetric Q-Ising neural networks

D. Bollé *† and G. Jongen *†
Instituut voor Theoretische Fysica, K.U. Leuven,
B-3001 Leuven, Belgium

and G. M. Shim ‡
Department of Physics, Chungnam National University
Yuseong, Taejon 305-764, R.O. Korea

Abstract

The parallel dynamics of extremely diluted *symmetric* Q-Ising neural networks is studied for arbitrary Q using a probabilistic approach. In spite of the extremely diluted architecture the feedback correlations arising from the symmetry prevent a closed-form solution in contrast with the extremely diluted *asymmetric* model. A recursive scheme is found determining the complete time evolution of the order parameters taking into account *all* feedback. It is based upon the evolution of the distribution of the local field, as in the fully connected model. As an illustrative example an explicit analysis is carried out for the $Q = 2$ and $Q = 3$ model. These results agree with and extend the partial results existing for $Q = 2$. For $Q > 2$ the analysis is entirely new. Finally, equilibrium fixed-point equations are derived and a capacity-gain function diagram is obtained.

Key words: Extremely diluted symmetric networks; Q-Ising neurons; parallel dynamics; probabilistic approach

*e-mail: {desire.bolle, greetje.jongen}@fys.kuleuven.ac.be.
†Also at Interdisciplinair Centrum voor Neurale Netwerken, K.U.Leuven, Belgium.
‡e-mail: gmshim@nsphys.chungnam.ac.kr.

1 Introduction

For the parallel dynamics of extremely diluted asymmetric and layered feed-forward $Q \geq 2$-Ising neural networks recursion relations for the relevant order parameters have been obtained in closed form (cfr. [1]-[4] and the references cited therein). This has been possible because in these types of networks one knows that there are no feedback correlations as time progresses.

For the parallel dynamics of networks with symmetric connections, however, things are quite different. Even for extremely diluted versions of these systems it is known that feedback correlations become essential from the second time step onwards, complicating the dynamics in a nontrivial way. As a consequence explicit results concerning the time evolution of the retrieval overlap for these symmetrically diluted models have been obtained for the $Q = 2$ case up to the third time step only [5]-[6]. Furthermore, the local instability of neighbouring trajectories has been examined, recently, invoking the ansatz that the second step formula for the retrieval overlap stays valid for all times $t \geq 2$ [7]. So, up to now, no systematic analytic procedure is available, even for $Q = 2$, for calculating the complete time evolution taking into account *all* feedback correlations. The main purposes of this paper are to fill this gap and extend the results to general Q.

The method used is a probabilistic signal-to-noise analysis [8] but starting from the distribution of the local field instead of working directly with the order parameters. Recently, a complete solution for the parallel dynamics of fully connected Q-Ising networks at zero-temperature has been obtained in this way [9]. Similar to the fully connected architecture, and in contrast with the extremely diluted asymmetric and layered network architectures, the local field contains both a discrete and a normally distributed part. The difference with the fully connected model is that the discrete part at a certain time t does not involve the spins at all previous times $t-1, t-2, \ldots$ up to 0 but only the spins at time step $t-1$. But, again this discrete part prevents a closed-form solution of the dynamics. Nevertheless, we succeed in developing a recursive scheme in order to calculate the complete time evolution of the order parameters – the retrieval overlap and the activity – taking into account all feedback correlations. In this way we have completed our discussion of the parallel dynamics at zero temperature for the different architectures – asymmetric and symmetric extremely diluted, layered feedforward and fully connected – considered in the literature.

As an illustration we write out these expressions in detail for the first five time steps of the dynamics. For $Q = 2$ our results agree with the first three time steps available in the literature [5]-[6] and extend these by a systematic analytic

procedure. Furthermore we find that the ansatz put forward in [7] strongly overestimates the retrieval overlap. For $Q \geq 3$ our results are new and do give a clear picture of the evolution of the network in the retrieval regime.

Finally, by requiring the local field to become time-independent implying that some correlations between its Gaussian and discrete noise parts are neglected we can obtain fixed-point equations for the order parameters. For $Q = 2$ they coincide with those derived via thermodynamical methods [10]. For $Q \geq 3$ they are not given in the literature before. In this case we obtain for the first time the structure of the capacity-gain parameter diagram.

The rest of the paper is organized as follows. In Section 2 we introduce the model, its dynamics and the Hamming distance as a macroscopic measure for the retrieval quality. In Section 3 we use the probabilistic approach in order to derive a recursive scheme for the evolution of the distribution of the local field, leading to recursion relations for the order parameters of the model. The differences with other architectures are outlined. Using this general scheme, we explicitly calculate in the Appendix the order parameters for the first five time steps of the dynamics. In Section 4 we discuss the evolution of the system to fixed-point attractors. For $Q = 2, 3$ a detailed discussion of the theoretical results obtained in Section 3 and the Appendix is presented in Section 5. Some concluding remarks are given in Section 6.

2 The model

Consider a neural network Λ consisting of N neurons which can take values σ_i from a discrete set $\mathcal{S} = \{-1 = s_1 < s_2 < \ldots < s_Q = +1\}$. The p patterns to be stored in this network are supposed to be a collection of independent and identically distributed random variables (i.i.d.r.v.), $\{\xi_i^\mu \in \mathcal{S}\}$, $\mu \in \mathcal{P} = \{1, \ldots, p\}$ and $i \in \Lambda$, with zero mean, $E[\xi_i^\mu] = 0$, and variance $A = \mathrm{Var}[\xi_i^\mu]$. The latter is a measure for the activity of the patterns. Given the configuration $\boldsymbol{\sigma}_\Lambda(t) \equiv \{\sigma_j(t)\}, j \in \Lambda = \{1, \ldots, N\}$, the local field in neuron i equals

$$h_i(\boldsymbol{\sigma}_{\Lambda\setminus\{i\}}(t)) = \sum_{j \in \Lambda\setminus\{i\}} J_{ij}\sigma_j(t) \tag{1}$$

with J_{ij} the synaptic couplings between neurons i and j. In the sequel we write the shorthand notation $h_{\Lambda,i}(t) \equiv h_i(\boldsymbol{\sigma}_{\Lambda\setminus\{i\}}(t))$.

The network is taken to be extremely diluted but symmetric meaning that the couplings are chosen as follows. Let $\{c_{ij} = 0, 1\}, i, j \in \Lambda$ be i.i.d.r.v. with distri-

bution $\Pr\{c_{ij}=x\}=(1-C/N)\delta_{x,0}+(C/N)\delta_{x,1}$ and satisfying $c_{ij}=c_{ji},\;\; c_{ii}=0$, then

$$J_{ij}=\frac{c_{ij}}{CA}\sum_{\mu\in\mathcal{P}}\xi_i^\mu\xi_j^\mu \quad \text{for} \quad i\neq j\,. \tag{2}$$

Compared with the asymmetrically diluted model [11] the architecture is still a local Cayley-tree but no longer directed and in the limit $N\to\infty$ the probability that the number of connections $T_i=\{j\in\Lambda|c_{ij}=1\}$ giving information to the site $i\in\Lambda$ is still a Poisson distribution with mean $C=E[|T_i|]$. Thereby it is assumed that $C\ll\log N$ and in order to get an infinite average connectivity allowing to store infinitely many patterns p one also takes the limit $C\to\infty$ and defines the capacity α by $p=\alpha C$. However, although for the asymmetric architecture, at any given time step t all spins are uncorrelated and hence no feedback is present; for the symmetric architecture this is no longer the case, causing a feedback from $t\geq 2$ onwards [6]. This feedback complicates the dynamics.

The following dynamics is considered. The configuration $\boldsymbol{\sigma}_\Lambda(t=0)$ is chosen as input. At zero temperature all neurons are updated in parallel according to the rule

$$\sigma_i(t)\to\sigma_i(t+1)=s_k:\min_{s\in\mathcal{S}}\epsilon_i[s|\boldsymbol{\sigma}_{\Lambda\setminus\{i\}}(t)]=\epsilon_i[s_k|\boldsymbol{\sigma}_{\Lambda\setminus\{i\}}(t)]\,. \tag{3}$$

Here the energy potential $\epsilon_i[s|\boldsymbol{\sigma}_{\Lambda\setminus\{i\}}]$ is defined by

$$\epsilon_i[s|\boldsymbol{\sigma}_{\Lambda\setminus\{i\}}]=-\frac{1}{2}[h_i(\boldsymbol{\sigma}_{\Lambda\setminus\{i\}})s-bs^2]\,, \tag{4}$$

where $b>0$ is the gain parameter of the system. The updating rule (3) is equivalent to using a gain function $\mathrm{g}_b(\cdot)$,

$$\begin{aligned}\sigma_i(t+1) &= \mathrm{g}_b(h_{\Lambda,i}(t))\\ \mathrm{g}_b(x) &\equiv \sum_{k=1}^{Q}s_k\left[\theta\left[b(s_{k+1}+s_k)-x\right]-\theta\left[b(s_k+s_{k-1})-x\right]\right]\end{aligned} \tag{5}$$

with $s_0\equiv-\infty$ and $s_{Q+1}\equiv+\infty$. For finite Q, this gain function $\mathrm{g}_b(\cdot)$ is a step function. The gain parameter b controls the average slope of $\mathrm{g}_b(\cdot)$.

To measure the retrieval quality of the system one can use the Hamming distance between a stored pattern and the microscopic state of the network

$$d(\boldsymbol{\xi}^\mu,\boldsymbol{\sigma}_\Lambda(t))\equiv\frac{1}{N}\sum_{i\in\Lambda}[\xi_i^\mu-\sigma_i(t)]^2\,. \tag{6}$$

This naturally introduces the main overlap

$$m^\mu_\Lambda(t) = \frac{1}{NA}\sum_{i\in\Lambda}\xi^\mu_i \sigma_i(t) \quad \mu \in \mathcal{P} \tag{7}$$

and the arithmetic mean of the neuron activities

$$a_\Lambda(t) = \frac{1}{N}\sum_{i\in\Lambda}[\sigma_i(t)]^2 \,. \tag{8}$$

We recall that in the thermodynamic limit $C, N \to \infty$ all averages will have to be taken over the treelike structure, viz. $\frac{1}{N}\sum_{i\in\Lambda} \to \frac{1}{C}\sum_{i\in T_j}$. We remark that for $Q = 2$ the variance of the patterns $A = 1$, and the neuron activity $a_\Lambda(t) = 1$.

3 Recursive dynamical scheme

As mentioned above in an extremely diluted network the symmetric couplings cause non-trivial correlations, even at zero temperature, which are known to become increasingly tedious to evaluate [5]-[6]. So, results on the dynamics for these symmetric systems existing up to now concern $Q = 2$ only and are restricted to the first three time steps.

Using a probabilistic approach (see, e.g.,[4],[8]) we calculate the distribution of the local field for a general time step for $Q \geq 2$ systems analogously to the fully connected case studied very recently [9]. This allows us to obtain recursion relations determining the full time evolution of the relevant order parameters.

Suppose that the initial configuration of the network $\{\sigma_i(0)\}, i \in \Lambda$, is a collection of i.i.d.r.v. with mean $\mathrm{E}[\sigma_i(0)] = 0$, variance $\mathrm{Var}[\sigma_i(0)] = a_0$, and correlated with only one stored pattern, say the first one $\{\xi^1_i\}$:

$$\mathrm{E}[\xi^\mu_i \sigma_j(0)] = \delta_{i,j}\delta_{\mu,1} m^1_0 A \quad m^1_0 > 0 \,. \tag{9}$$

This implies that by the law of large numbers (LLN) one gets for the main overlap and the activity at $t = 0$

$$m^1(0) \equiv \lim_{C,N\to\infty} m^1_\Lambda(0) \overset{Pr}{=} \frac{1}{A}\mathrm{E}[\xi^1_i \sigma_i(0)] = m^1_0 \tag{10}$$

$$a(0) \equiv \lim_{C,N\to\infty} a_\Lambda(0) \overset{Pr}{=} \mathrm{E}[\sigma^2_i(0)] = a_0 \tag{11}$$

where the convergence is in probability [12]. Writing the local field at $t = 0$ as

$$h_i(0) = \lim_{C,N\to\infty}\left[\xi_i^1 m_{T_i}^1(0) + \frac{1}{CA}\sum_{\mu\in\mathcal{P}\setminus\{1\}}\sum_{j\in T_i}\xi_i^\mu\xi_j^\mu\sigma_j(0)\right] \tag{12}$$

where

$$m_{T_j}^\mu(t) \equiv \frac{1}{CA}\sum_{i\in T_j}\xi_i^\mu\sigma_i(t) \tag{13}$$

and where we recall that T_j is the part of the tree connected to neuron j, we find using standard signal-to-noise techniques (see, e.g., [6],[11])

$$h_i(0) \stackrel{\mathcal{D}}{=} \xi_i^1 m^1(0) + \mathcal{N}(0, \alpha a_0)\,, \tag{14}$$

where the convergence is in distribution [12]. The quantity $\mathcal{N}(0, V)$ represents a Gaussian random variable with mean 0 and variance V. At this point we note that this structure of the distribution of the local field at time zero – signal plus Gaussian noise – is typical for all architectures treated in the literature.

The key question is then how these quantities evolve in time under the parallel dynamics specified before. For a general time step we find from eq. (5) and the LLN in the limit $C, N \to \infty$ for the main overlap (7) and the activity (8)

$$m^1(t+1) \stackrel{Pr}{=} \frac{1}{A}\langle\!\langle \xi_i^1 \mathrm{g}_b(h_i(t))\rangle\!\rangle \tag{15}$$

$$a(t+1) \stackrel{Pr}{=} \langle\!\langle \mathrm{g}_b^2(h_i(t))\rangle\!\rangle \tag{16}$$

with $h_i(t) \equiv \lim_{C,N\to\infty} h_{\Lambda,i}(t)$. In the above $\langle\!\langle\cdot\rangle\!\rangle$ denotes the average both over the distribution of the embedded patterns $\{\xi_i^\mu\}$ and the initial configurations $\{\sigma_i(0)\}$. The average over the initial configurations is hidden in an average over the local field through the updating rule (5).

From the work on fully connected networks [9] we know that due to the correlations we have to study carefully the influence of the non-condensed patterns in the time evolution of the system, expressed by the variance of the residual overlaps. The latter is defined as

$$r^\mu(t) \equiv \lim_{C,N\to\infty} r_{T_i}^\mu(t) = \lim_{C,N\to\infty}\frac{1}{A\sqrt{C}}\sum_{j\in T_i}\xi_j^\mu\sigma_j(t) \quad \mu\in\mathcal{P}\setminus\{1\}\,. \tag{17}$$

The aim of this section is then to calculate the distribution of the local field and the order parameters as a function of time. This can be done for arbitrary

Q without making the notation much heavier. The simplifications for $Q = 2$ will be mentioned when appropriate.

We start by rewriting the local field (1) at time t in the following way

$$h_{\Lambda,i}(t) = \xi_i^1 m_{T_i}^1(t) + \frac{1}{\sqrt{C}} \sum_{\mu \in \mathcal{P}\setminus\{1\}} \xi_i^\mu r_{T_i}^\mu(t)\,. \tag{18}$$

We first concentrate on the residual overlap $r_{T_i}^\mu(t)$, $\mu \in \mathcal{P}\setminus\{1\}$. Since the neurons $\{\sigma_j(t)|j \in T_i\}$ are not i.i.d.r.v. the central limit theorem (CLT) can not be applied directly to this residual overlap. Therefore we follow a procedure similar to that used for the fully connected model [9] by taking out of the local field precisely the contributions arising from these dependences. In order to do so we apply the dynamics writing the residual overlap (17) as

$$r_{T_i}^\mu(t+1) = \frac{1}{A\sqrt{C}} \sum_{j \in T_i} \xi_j^\mu \mathrm{g}_b \left(\xi_j^1 m_{T_j}^1(t) + \frac{1}{\sqrt{C}} \sum_{\nu \in \mathcal{P}\setminus\{1\}} \xi_j^\nu r_{T_j}^\nu(t) \right)\,. \tag{19}$$

In analogy with the fully connected case we expect contributions coming from the fact that the $\sigma_j(t+1)$ are dependent on the $\sigma_i(t)$ for all $j \in T_i$ and from the fact that the $\sigma_j(t+1)$ and ξ_j^μ are dependent (the latter dependence is microscopic but leads, at least for a fully connected architecture, to a macroscopic contribution in the thermodynamic limit). Therefore, we define a modified local field

$$\hat{h}_{\Lambda,j}^\mu(t) = \xi_j^1 m_{T_j}^1(t) + \frac{1}{\sqrt{C}} \sum_{\nu \in \mathcal{P}\setminus\{1,\mu\}} \xi_j^\nu r_{T_j}^\nu(t)\,. \tag{20}$$

Expanding $\mathrm{g}_b(\cdot)$ in (19) around $\hat{h}_{\Lambda,j}^\mu(t)$ we arrive at

$$\begin{aligned} r_{T_i}^\mu(t+1) &= \frac{1}{A\sqrt{C}} \sum_{j \in T_i} \xi_j^\mu \mathrm{g}_b(\hat{h}_{\Lambda,j}^\mu(t)) \\ &+ \frac{1}{A\sqrt{C}} \sum_{k=1}^{Q-1} \sum_{j \in T_i} \xi_j^\mu \Theta \left[|\frac{1}{\sqrt{C}} \xi_j^\mu r_{T_j}^\mu(t)| - |b(s_k + s_{k+1}) - \hat{h}_{\Lambda,j}^\mu(t)| \right] \\ &\times \frac{s_{k+1} - s_k}{2} \left[\mathrm{sign}(b(s_k + s_{k+1}) - \hat{h}_{\Lambda,j}^\mu(t)) + \mathrm{sign}(\frac{1}{\sqrt{C}} \xi_j^\mu r_{T_j}^\mu(t)) \right]\,, \end{aligned} \tag{21}$$

with Θ the Heaviside function. At this point we remark that instead of using explicitly the set of indices I_k where the term $\frac{1}{\sqrt{C}} \xi_j^\mu r_{T_j}^\mu(t)$ becomes relevant in the

gain function $g_b(\cdot)$ (see [9] for more details), we replace it, more conveniently, by the sum over j of the Heaviside function.

We then consider the limit $C, N \to \infty$. First we remark that in this limit the density distribution of the modified local field $\hat{h}_i^\mu(t)$ at time t equals the density distribution of the local field $h_i(t)$ itself. Hence, applying the CLT to the first term of (21) gives, recalling eqs. (16) and (20)

$$\tilde{r}^\mu(t) \equiv \lim_{C,N\to\infty} \frac{1}{A\sqrt{C}} \sum_{j\in T_i} \xi_j^\mu g_b(\hat{h}^\mu_{\Lambda,j}(t)) \ \stackrel{\mathcal{D}}{=}\ \mathcal{N}(0, a(t+1)/A) \tag{22}$$

because of the weak dependence of $\hat{h}_j^\mu(t)$ and ξ_j^μ. To the second term of (21) we apply the LLN arriving at a contribution given by the average of

$$\frac{1}{2\sqrt{C}} f'_{\hat{h}_j^\mu(t)}(b(s_{k+1}+s_k))\xi_j^\mu|\xi_j^\mu|^2(r^\mu_{T_j}(t))^2 + \chi(t)|\xi_j^\mu|^2 r^\mu_{T_j}(t) \tag{23}$$

over $\{\xi_j^\mu\}, \{\sigma_j(0)\}$ and where

$$\chi(t) = \sum_{k=1}^{Q-1}(s_{k+1}-s_k) f_{\hat{h}_j^\mu(t)}(b(s_{k+1}+s_k))\,. \tag{24}$$

Here $f_{\hat{h}_i^\mu(t)}$ is the probability density of the modified local field $\hat{h}_i^\mu(t)$ at time t and $f'_{\hat{h}_i^\mu(t)}$ denotes its derivative w.r.t. the argument. Since the residual overlap $r^\mu_{T_j}(t)$ depends explicitly on j, it is also averaged over, while in the fully connected case the residual overlap $r^\mu_\Lambda(t)$ is kept fixed. Doing these averages none of these terms contribute to $r^\mu(t+1)$ as expressed by (21).

This implies that $r^\mu(t+1)$ is Gaussian with variance $a(t+1)/A$, in contrast with both the fully connected architecture [9] and the layered architecture [4], where the variance contains extra terms. This finishes the treatment of the residual overlap. We remark that for $Q = 2$ the following simplifications are possible: $b(s_{k+1}+s_k) = 0, (s_{k+1}-s_k) = 2,\ g_b(\cdot) = \mathrm{sign}(\cdot)$ and $a(t) = A = 1$.

However, subtleties arise in the treatment of the local field at time $t+1$. We have to take into account the correlations between ξ_i^μ and $r^\mu_{T_i}$. Starting from the form (18) and using eqs. (21)-(23) we find that the second part of (23) leads to a contribution from the site i in the local field $h_i(t+1)$ given by $\alpha\chi(t)\sigma_i(t)$. This is different from the asymmetrically diluted case, where the probability to find the site i in $r^\mu_{T_j}$ is zero such that we do not get any contribution at all. Furthermore, for the fully connected case, where all sites of the residual overlap in the second

part of (23) are relevant, the latter leads to an extra contribution $\chi(t)h_i(t)$ in the local field $h_i(t+1)$.

So we obtain in the limit $C, N \to \infty$

$$h_i(t+1) = \xi_i^1 m^1(t+1) + \alpha\chi(t)\sigma_i(t) + \mathcal{N}(0, \alpha a(t+1))\,. \tag{25}$$

From this it is clear that the local field at time t consists out of a signal term, a discrete noise part and a normally distributed noise part. The variance of the local field is αA times the variance of the residual overlap. Furthermore, the discrete noise and the normally distributed noise are correlated and this prohibits us to derive a closed expression for the overlap and activity (eqs. (15)-(16)).

These correlations, which become more complicated as time evolves, will determine the distribution of the local field, $f_{h_i(t)}$ in eq. (24). Using the evolution equation $\sigma_i(t)$ can be replaced by $g_b(h_i(t-1))$ such that the discrete noise part is a stepfunction of correlated variables. These are correlated through the dynamics with the normally distributed part of $h_i(t)$. Therefore the local field can be considered as a transformation of a set of correlated normally distributed variables x_s, $s = t-2[t/2], \ldots, t-4, t-2, t$, which we choose to normalize. The brackets $[t/2]$ denote the integer part of $t/2$. Defining the correlation matrix $w \equiv (\rho(s,s')) = (E[x_s x_{s'}])$ we arrive at the following expression for the probability density of the local field at time t

$$\begin{aligned} f_{h_i(t)}(y) \;&=\; \int \prod_{s=0}^{[t/2]} dx_{t-2s}\; \delta\left(y - \xi_i^1 m^1(t) - \alpha\chi(t)\sigma_i(t) - \sqrt{\alpha a(t)}\, x_t\right) \\ &\times\; \frac{1}{\sqrt{\det(2\pi w)}} \exp\left(-\frac{1}{2}\mathbf{x} w^{-1} \mathbf{x}^T\right) \end{aligned} \tag{26}$$

with $\mathbf{x} = (x_{t-2[t/2]}, \ldots x_{t-2}, x_t)$.

In conclusion, eqs. (15),(16) together with eqs. (24)-(26) form a recursive scheme in order to obtain the order parameters of the system.

As an illustration we write down in the Appendix the evolution equations for the order parameters of a general $Q \geq 2$-Ising network for the first five time steps, taking into account all correlations. Five time steps suffice to give an accurate picture of the dynamics in the retrieval regime of the network as we will see in Section 5. In the literature only the first three time steps of the $Q = 2$ model are known. Our results completely solve the parallel dynamics for any $Q \geq 2$. This also allows us to determine precisely the effects of neglecting the correlations between the Gaussian and discrete part of the noise, i.e., an overestimate of the main overlap.

4 Fixed-point equations

A second type of results can be obtained by requiring through the recursion relations (25) that the local field becomes time-independent. This means that some of the discrete noise part is neglected. We show that for $Q = 2$ this procedure leads to the same fixed-point equations as those found from a thermodynamic replica symmetric mean-field theory approach in [10]. For $Q > 2$, however, these fixed-point equations are new since no replica results are available in the literature.

In the extremely diluted and layered Q-Ising models the evolution equations for the order parameters do not change their form as time progresses, such that the fixed-point equations are obtained immediately by leaving out the time dependence (see [2],[4]). This still allows small fluctuations in the configurations $\{\sigma_i\}$. Similar to the fully connected model the form of the evolution equations for the order parameters in the symmetrically diluted model treated here does change by the explicit appearance of the $\{\sigma_i(t)\}$ term, such that we can not use that procedure to obtain the fixed-point equations. Instead we require that the distribution of the local field given by (25) becomes independent of time. This is an approximation because fluctuations in the network configuration are no longer allowed. It implies that the main overlap and activity in the fixed-point are found from the definitions (7), (8) and not from leaving out the time dependence in the recursions relation (15) and (16).

So, eliminating the time-dependence in the evolution equations for the local field (25) one obtains

$$h_i = \xi_i^1 m^1 + \mathcal{N}(0, \alpha a) + \alpha\chi\sigma_i \tag{27}$$

with $h_i \equiv \lim_{t\to\infty} h_i(t)$. Employing this expression in the updating rule (5) one finds

$$\sigma_i = \mathrm{g}_b(\tilde{h}_i + \alpha\chi\sigma_i) \tag{28}$$

where $\tilde{h}_i = \mathcal{N}(\xi_i^1 m^1, \alpha a)$ is the normally distributed part of eq. (27). Compared with the fully connected model (see [9] eqs. (79) and (80)) one sees that the equations here have a similar structure but simpler coefficients in front of the noise terms, viz. the denominator $1 - \chi$ is replaced by 1. Therefore the same method of solution as in the fully connected case, i.e., a geometrical Maxwell construction (see also [13],[14]) can be employed.

To make the discussion self-contained we shortly recall this method. Let L be the straight line which connects the centers of the plateaus of the gain function

$\mathrm{g}_b(\cdot)$. The equations for the functions $\mathrm{g}_b(\cdot)$ and $L(\cdot)$ read

$$\begin{aligned} \mathrm{g}_b \quad &: \quad x \mapsto s_k \text{ if } b(s_k + s_{k-1}) < x < b(s_k + s_{k+1}) && (29)\\ L \quad &: \quad x \mapsto \frac{x}{2b}\,. && (30) \end{aligned}$$

The condition on the r.h.s. of (29) is a condition on x. Using the definition of $L(\cdot)$, one can transform this into a condition on the image of $L(\cdot)$, $\mathcal{I}_L = \{y \in \mathbb{R} \,|\, \exists\, x \in \mathbb{R} : L(x) = y\}$, viz.

$$\mathrm{g}_b(x) = s_k \text{ if } \frac{s_k + s_{k-1}}{2} < L(x) < \frac{s_k + s_{k+1}}{2}\,. \tag{31}$$

Consider the transformation $\mathcal{T} : (x, y) \mapsto (x - \alpha\chi y, y)$

$$\mathcal{T}(L) : x \mapsto \frac{x}{2(b - \frac{\alpha\chi}{2})}\,. \tag{32}$$

The function $\mathcal{T}(\mathrm{g}_b)(\cdot)$ is not bijective while $\mathcal{T}$ is not one-to-one. To obtain a unique solution for eq. (28) we modify the former function such that it becomes a step function with the same step height as the one in $\mathcal{T}(\mathrm{g}_b)(\cdot)$ and the width of the steps such that $\mathcal{T}(L)$ connects the centers of the plateaus:

$$\mathcal{T}_L(\mathrm{g}_b)(x) = s_k \text{ if } (b - \frac{\alpha\chi}{2})(s_k + s_{k-1}) < x < (b - \frac{\alpha\chi}{2})(s_k + s_{k+1}) \tag{33}$$

or, using (5)

$$\mathcal{T}_L(\mathrm{g}_b)(x) = \mathrm{g}_{\tilde{b}}(x) \text{ with } \tilde{b} = b - \frac{\alpha\chi}{2}\,. \tag{34}$$

This at first sight ad-hoc modification leads us to a unique solution of the self-consistent equation (28). Indeed, from this modified transformation we know that

$$\mathrm{g}_b(\tilde{h} + \alpha\chi\sigma) \simeq \mathrm{g}_{\tilde{b}}(\tilde{h} + \alpha\chi\sigma - \alpha\chi\mathrm{g}_b(\tilde{h} + \alpha\chi\sigma))\,, \tag{35}$$

such that

$$\sigma_i = \mathrm{g}_{\tilde{b}}(\tilde{h}_i)\,. \tag{36}$$

Using the definition of the main overlap and activity (7) and (8) in the limit $C, N \to \infty$, one finds in the fixed point

$$\begin{aligned} m^1 \quad &= \quad \frac{1}{A}\left\langle\!\!\left\langle \xi^1 \int \mathcal{D}z \; \mathrm{g}_{\tilde{b}}\left(\xi^1 m^1 + \sqrt{\alpha a}\, z\right)\right\rangle\!\!\right\rangle && (37)\\ a \quad &= \quad \left\langle\!\!\left\langle \int \mathcal{D}z \; \mathrm{g}_{\tilde{b}}^2\left(\xi^1 m^1 + \sqrt{\alpha a}\, z\right)\right\rangle\!\!\right\rangle\,, && (38) \end{aligned}$$

where we recall that

$$\tilde{b} = b - \frac{\alpha\chi}{2}, \quad \chi = \frac{1}{\sqrt{\alpha a}} \left\langle\!\!\left\langle \int \mathcal{D}z \; z\, \mathrm{g}_{\tilde{b}}\left(\xi^1 m^1 + \sqrt{\alpha a}\, z\right) \right\rangle\!\!\right\rangle . \tag{39}$$

For the special case of $Q = 2$ the resulting equations (37)-(39) are the same as those derived from a thermodynamic replica-symmetric mean-field theory treatment in [10]. For general $Q > 2$ such a comparison can not be made because a thermodynamic treatment is not yet available in the literature. Hence it is interesting to write down these equations in more detail here

$$m = \frac{s_1 + s_Q}{2A} \left\langle\!\!\left\langle \xi^1 \right\rangle\!\!\right\rangle + \frac{1}{2A} \sum_{k=1}^{Q-1} (s_{k+1} - s_k) \left\langle\!\!\left\langle \xi^1 \mathrm{erf}\left(\frac{\xi^1 m^1 - \tilde{b}(s_{k+1} + s_k)}{\sqrt{\alpha a}} \right) \right\rangle\!\!\right\rangle \tag{40}$$

$$a = \frac{s_1^2 + s_Q^2}{2} \left\langle\!\!\left\langle \xi^1 \right\rangle\!\!\right\rangle + \frac{1}{2} \sum_{k=1}^{Q-1} (s_{k+1}^2 - s_k^2) \left\langle\!\!\left\langle \mathrm{erf}\left(\frac{\xi^1 m^1 - \tilde{b}(s_{k+1} + s_k)}{\sqrt{\alpha a}} \right) \right\rangle\!\!\right\rangle \tag{41}$$

$$\chi = \frac{1}{\sqrt{2\pi\alpha a}} \left\langle\!\!\left\langle \sum_{k=1}^{Q-1} (s_{k+1} - s_k) \exp \frac{-\left(\xi^1 m^1 - \tilde{b}(s_{k+1} + s_k)\right)^2}{2\alpha a} \right\rangle\!\!\right\rangle \tag{42}$$

$$\tilde{b} = b - \frac{\alpha\chi}{2} . \tag{43}$$

We are presently working out such a thermodynamic approach for these systems at arbitrary temperature [15].

5 Numerical results

The equations derived in Section 3 and the Appendix have been studied numerically for the $Q = 2, 3$ model with equidistant states and a uniform distribution of patterns, implying that $A = 1$ for $Q = 2$ and $A = 2/3$ for $Q = 3$.

In the $Q = 2$ case the temperature-capacity phase diagram given by a thermodynamic replica-symmetric mean-field theory approach has been presented in [10]. From that work we know that the critical capacity at zero temperature equals 0.634. So we discuss the parallel dynamics using the complete recursive scheme developed here for a typical point in the retrieval regime, e.g., $\alpha = 0.3$. In Fig. 1 we show the overlap $m^1(t), t = 1$ to 5 versus the initial overlap m_0^1 with the condensed pattern (thick lines). (We forget about the superscript 1). For $m_0 \geq 0.4$ we see that the retrieval attractor is reached quickly. In fact four or five time steps give us already an accurate picture of the dynamics in the retrieval

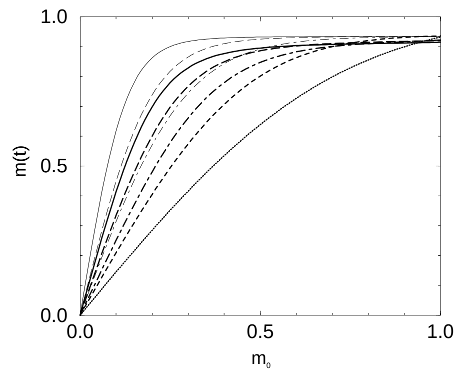

Figure 1: The overlap $m(t)$ for $Q = 2$ systems is presented for the first five time steps as a function of m_0 for $\alpha = 0.3$. The results for the first, second, third, fourth and fifth time step are indicated by a dotted, a short-dashed, a dashed-dotted, a long-dashed and a full curve respectively. The results using the ansatz of ref. [7] for the third, fourth and fifth time step are indicated with thin lines.

region. At this point we note that the convergence to the attractor is of an oscillating nature, in contrast with the asymmetrically diluted model. The first three time steps were given in the literature before ([5]-[6]) and they agree completely with our results.

In this figure we also indicate the overlap (thin lines) when making the ansatz [7] that the structure of the formula for the second time step is valid for any time step. This ansatz neglects some correlations and it systematically overestimates the overlap for all m_0. This effect becomes even stronger when going from time step 3 to 5.

Concerning the $Q = 3$ model, in order to determine the retrieval regime of the network, we first have to solve the fixed-point equations (40)-(43) derived in Section 4 since a thermodynamic phase diagram is not available in the literature. The resulting capacity-gain diagram is presented in Fig. 2. We discover three different regions in the retrieval regime. In region I (bounded by the straight full line and the dashed-dotted line) the activity a is of order 1, and $\tilde{b} \leq 0$. Consequently we call it the Ising-like region. In region II and III, a is of order A (and $\tilde{b} > 0$). The difference between II and III, separated by a short-dashed line, is that there is no sustained activity state ($m = 0, a \neq 0$) present in the latter. The zero solution is always a fixed-point. We remark that the boundary of the retrieval region is denoted by a full line when the transition (to the spin-

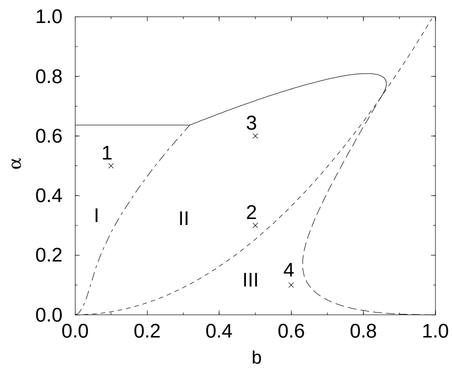

Figure 2: The $\alpha - b$ phase diagram for $Q = 3$. The full curve and long-dashed curve indicate the boundary of the retrieval region. The dashed-dotted curve denotes the boundary between the Ising-like region I and the other regions. The short-dashed curve represents the boundary between regions II and III. The points 1 to 4 indicate the network parameters used in the discussion of the dynamics.

glass phase) is continuous and by a broken line when it is first-order. For further details on this diagram, which are not relevant to our present discussion we refer to [15].

For specific network parameters corresponding to some arbitrarily chosen points in the retrieval phase in this equilibrium phase diagram, indicated as 1 to 4, we have studied the dynamics governed by the evolution equations found here. Figures 3-5 present an overview of these results by plotting the overlap $m(t)$, the activity $a(t)$ and the Hamming distance $d(t)$ versus the initial overlap m_0 with the condensed pattern. The initial activity is taken to be $a_0 = 0.83$.

In the Ising-like region I, the network parameters corresponding to point 1 are $\alpha = 0.5, b = 0.1$. We see in Fig. 3 that the Hamming distance, $d(t)$, reaches its plateau value indicating retrieval for $m_0 > 0.6$. The corresponding value of the main overlap is about 0.83 and the activity goes to values larger than $A = 2/3$. So, the network configuration is no longer uniformly distributed: the state $\sigma_i = 0$ has a smaller probability to appear than the states $\sigma_i = \pm 1$. Hence, the Hamming distance can never be that small.

A somewhat similar type of behavior is found in the fully connected model in the region where the order parameter giving the mean-square random overlap with the non-condensed patterns is of order 10 [9].

For a network corresponding to point 2 in region II of the phase diagram

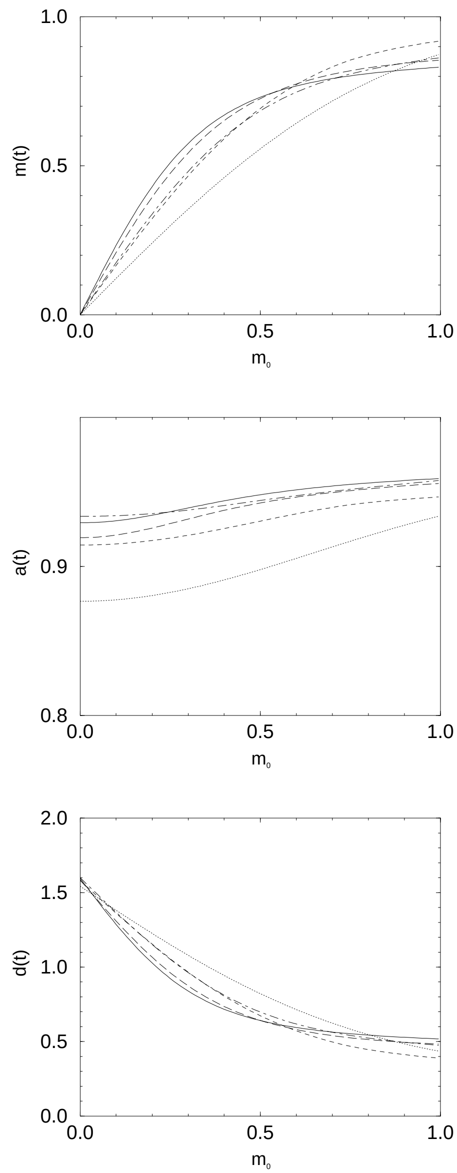

Figure 3: The overlap $m(t)$, the activity $a(t)$ and the Hamming distance $d(t)$ are presented for the first five time steps as a function of m_0 for the network parameters $b = 0.1, \alpha = 0.5, a_0 = 0.83$. The curves for the different time steps are as in Fig. 1

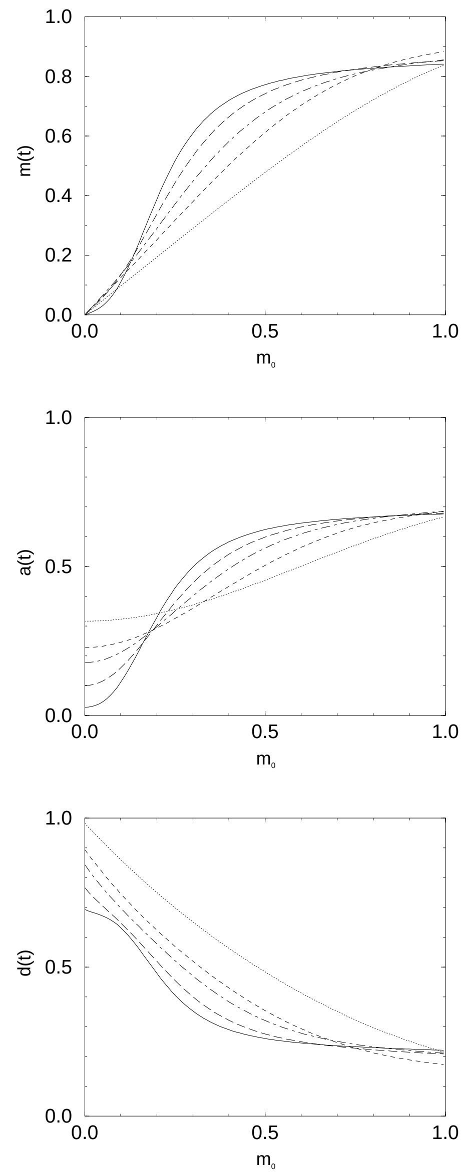

Figure 4: As in Fig. 3, for the network parameters $b = 0.5, \alpha = 0.3, a_0 = 0.83$.

with $\alpha = 0.3, b = 0.5$ we see in Fig. 4 that for $m_0 > 0.5$ the dynamics evolves to the retrieval attractor with main overlap $m = 0.84$. For these values of m_0 the Hamming distance quickly goes to its plateau value (smaller than the one

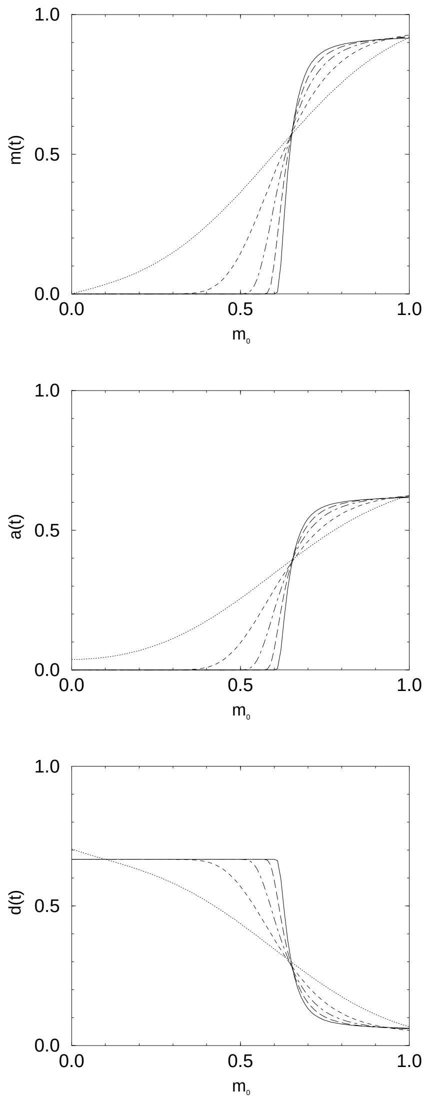

Figure 5: As in Fig. 3, for the network parameters $b = 0.6, \alpha = 0.1, a_0 = 0.83$.

of point 1). The activity then attains a value near A meaning that the network configuration is uniformly distributed. We remark that the boundary between the retrieval attractor and the zero attractor becomes clearly visible, especially in the behavior of $m(t)$ and $a(t)$. In this region we have also considered the point labeled as 3, i.e., $\alpha = 0.6, b = 0.5$. There the behavior of the dynamics is very

similar to point 1, and hence we have not drawn a corresponding figure, except for the fact that the activity a goes to a value near A (as for point 2) indicating again a uniformly distributed network configuration.

In region III of the phase diagram for the network parameters corresponding to point 4 with $\alpha = 0.1, b = 0.6$, we need a greater value of m_0 to reach the retrieval attractor. As seen in Fig. 5, m_0 has to be at least 0.65. But the value of the main overlap is larger, $m = 0.93$, and the Hamming distance is smaller than for the other network parameters. Furthermore, the boundary between the retrieval attractor and the zero-attractor is sharply determined.

6 Concluding remarks

An evolution equation is derived for the distribution of the local field governing the parallel dynamics at zero temperature of extremely diluted *symmetric* $Q \geq 2$-Ising networks. For the first time, *all* feedback correlations are taken into account. In contrast with extremely diluted asymmetric and layered networks and in analogy with fully connected models this distribution is no longer normally distributed but contains a discrete part.

Employing this evolution equation a general recursive scheme is developed allowing one to calculate the relevant order parameters of the system, i.e., the main overlap and the activity for *any* time step. This scheme has been worked out explicitly for the first five time steps of the dynamics.

Under the condition that the local field becomes time-independent, meaning also that some of the discrete noise part is neglected, fixed-point equations are obtained for these order parameters. For $Q > 2$ these equations were not given in the literature before. Hence, we have shortly discussed the capacity-gain diagram for the $Q = 3$ model.

As an illustration a detailed discussion of the dynamics is given for the $Q = 2$ and $Q = 3$ model. It is seen from these numerical results that the first four or five time steps do give already a clear picture of the time evolution in the retrieval regime of the network. For $Q = 2$ the ansatz that the structure of the formula for the second time step is valid for all times $t \geq 2$, neglecting any further correlations between the Gaussian and discrete part of the noise, strongly overestimates the retrieval overlap.

Acknowledgments

This work has been supported in part by the Research Fund of the K.U.Leuven (Grant OT/94/9) and the Korea Science and Engineering Foundation through the SRC program. The authors are indebted to G. Massolo, A. Patrick and V. Zagrebnov for constructive discussions. One of us (D.B.) thanks the Belgian National Fund for Scientific Research for financial support.

References

[1] B. Derrida, E. Gardner, and A. Zippelius, An exactly solvable asymmetric neural network model, *Europhys. Lett.* **4**:167 (1987).

[2] D. Bollé, G.M. Shim, B. Vinck, and V.A. Zagrebnov, Retrieval and chaos in extremely diluted Q-Ising neural networks, *J. Stat. Phys.* **74**: 565 (1994).

[3] E. Domany, W. Kinzel, and R. Meir, Layered neural networks, *J. Phys. A: Math. Gen.* **22**:2081 (1989).

[4] D. Bollé, G.M. Shim, and B. Vinck, Retrieval and chaos in layered Q-Ising neural networks, *J. Stat. Phys.* **74**: 583 (1994).

[5] T.L.H. Watkin and D. Sherrington, The parallel dynamics of a dilute symmetric neural network, *J. Phys. A: Math. Gen.* **24**: 5427 (1991).

[6] A.E. Patrick and V.A. Zagrebnov, Parallel dynamics for an extremely diluted neural network, *J. Phys. A: Math. Gen.* **23**: L1323 (1990); *J. Phys. A: Math. Gen.* **25**: 1009 (1992).

[7] D. Gandolfo, M. Sirugue-Collin and V.A. Zagrebnov, Local instability and oscillations of trajectories in a diluted symmetric neural network, to appear in *Neural Computation*.

[8] A.E. Patrick and V.A. Zagrebnov, On the parallel dynamics for the Little-Hopfield model, *J. Stat. Phys.* **63**: 59 (1991).

[9] D. Bollé, G. Jongen and G.M. Shim, Parallel dynamics of fully connected Q-Ising neural networks, *J. Stat. Phys.* **91**: 125 (1998).

[10] T.L.H. Watkin, and D. Sherrington, A neural network with low symmetric connectivity, *Europhys. Lett.* **14**: 791 (1991)

[11] D. Bollé, B. Vinck, and V.A. Zagrebnov, On the parallel dynamics of the Q-state Potts and Q-Ising neural networks, *J. Stat. Phys.* **70**: 1099 (1993).

[12] A.N. Shiryayev, *Probability* (Springer, New York, 1984).

[13] M. Shiino and T. Fukai, Self-consistent signal-to-noise analysis and its application to analogue neural networks with asymmetric connections, *J. Phys. A: Math. Gen.* **25**: L375 (1992).

[14] M. Shiino and T. Fukai, Self-consistent signal-to-noise analysis of the statistical behavior of analog neural networks and enhancement of the storage capacity, *Phys. Rev. E* **48**: 867 (1993).

[15] D. Bollé and G.M. Shim, Thermodynamic properties of extremely diluted symmetric Q-Ising neural networks, in preparation.

Appendix: Evolution equations for the first few time steps

A1: First step dynamics

The order parameters for the first time step can be written down immediately using eqs. (12),(15) and (16)

$$\begin{aligned} m^1(1) &= \frac{1}{A}\left\langle\!\!\left\langle \xi^1 \int \mathcal{D}z \; \mathrm{g}_b(\xi^1 m^1(0) + \sqrt{\alpha a(0)}\, z) \right\rangle\!\!\right\rangle & (44) \\ a(1) &= \left\langle\!\!\left\langle \int \mathcal{D}z \; \mathrm{g}_b^2(\xi^1 m^1(0) + \sqrt{\alpha a(0)}\, z) \right\rangle\!\!\right\rangle , & (45) \end{aligned}$$

where $\langle\!\langle \cdots \rangle\!\rangle$ now indicates the average taken with respect to the distribution of the first pattern and the initial configuration and $\mathcal{D}z$ denotes a Gaussian measure $\mathcal{D}z = dz \exp(-\frac{1}{2}z^2)/\sqrt{2\pi}$.

A2: Second step dynamics

First we need the distribution of the local field at time $t = 1$ which can be read off from eqs. (26)

$$h_i(1) = \xi_i^1 m^1(1) + \alpha\chi(0)\sigma_i(0) + \mathcal{N}(0, \alpha a(1)) \,. \tag{46}$$

with (see eq. (24))

$$\chi(0) = \left\langle\!\!\left\langle \frac{1}{\sqrt{\alpha a(0)}} \int \mathcal{D}z \; z \; \mathrm{g}_b(\xi^1 m^1(0) + \sqrt{\alpha a(0)}\, z) \right\rangle\!\!\right\rangle \,. \tag{47}$$

Recalling again eqs. (15) and (16), the main overlap and the activity read

$$\begin{aligned} m^1(2) &= \frac{1}{A}\left\langle\!\!\left\langle \xi^1 \int \mathcal{D}z \; \mathrm{g}_b\left(\xi^1 m^1(1) + \alpha\chi(0)\sigma(0) + \sqrt{\alpha a(1)}\, z\right) \right\rangle\!\!\right\rangle & (48) \\ a(2) &= \left\langle\!\!\left\langle \int \mathcal{D}z \; \mathrm{g}_b^2\left(\xi^1 m^1(0) + \alpha\chi(0)\sigma(0) + \sqrt{\alpha a(1)}\, z\right) \right\rangle\!\!\right\rangle & (49) \end{aligned}$$

A3: Third step dynamics

We start again by writing down the distribution of the local field at time $t = 2$.

$$h_i(2) = \xi_i^1 m^1(2) + \alpha\chi(1)\sigma_i(1) + \mathcal{N}(0, \alpha a(2)) \tag{50}$$

where (eqs. (24), (26))

$$\chi(1) = \frac{1}{\sqrt{\alpha a(1)}} \left\langle\!\!\left\langle \int \mathcal{D}z\, z\, \mathrm{g}_b\left(\xi^1 m^1(1) + \alpha\chi(0)\sigma(0) + \sqrt{\alpha a(1)}\, z\right)\right\rangle\!\!\right\rangle . \qquad (51)$$

This gives for the main overlap

$$m^1(3) = \frac{1}{A}\left\langle\!\!\left\langle \xi^1 \mathrm{g}_b\left(\xi^1 m^1(2) + \alpha\chi(1)\sigma(1) + \sqrt{\alpha a(2)}\, y\right)\right\rangle\!\!\right\rangle \qquad (52)$$

with y the Gaussian random variable $\mathcal{N}(0,1)$. The average has to be taken over $\xi^1, y,\ \sigma_i(0)$ and $\sigma_i(1)$. The average over ξ^1 and $\sigma_i(0)$ causes no difficulties because this initial configuration is chosen randomly. The average over y, the Gaussian random variable appearing in $h_i(2)$, and $\sigma_i(1)$ is more tricky because $h_i(2)$ and $\sigma_i(1)$ are correlated by the dynamics. However, the evolution equation (5) tells us that $\sigma_i(1)$ can be replaced by $\mathrm{g}_b(h_i(0))$ and, hence, the average can be taken over $h_i(0)$ instead of $\sigma_i(1)$.

From the recursion relation (25) one finds for the correlation coefficient between $h_i(0)$ and $h_i(2)$

$$\rho(2,0) = \frac{1}{\sqrt{a(0)a(2)}} \left\langle\!\!\left\langle \sigma(0) \int \mathcal{D}z\, \mathrm{g}_b\left(\xi^1 m^1(1) + \alpha\chi(0)\sigma(0) + \sqrt{\alpha a(1)}\, z\right)\right\rangle\!\!\right\rangle . \qquad (53)$$

Using all this the main overlap at the third time step (52) becomes

$$\begin{aligned} m^1(3) &= \frac{1}{A}\left\langle\!\!\left\langle \xi^1 \int \mathcal{D}w^{2,0}(x,y)\, \mathrm{g}_b\Big(\xi^1 m^1(2) + \right.\right. \\ &\qquad \left.\left. \alpha\chi(1)\left[\mathrm{g}_b(\xi^1 m^1(0) + \sqrt{\alpha a(0)}\, x)\right] + \sqrt{\alpha a(2)}\, y\Big)\right\rangle\!\!\right\rangle \end{aligned} \qquad (54)$$

where the joint distribution of x and y equals

$$\mathcal{D}w^{2,0}(x,y) = \frac{dx\ dy}{2\pi\sqrt{1-\rho(2,0)^2}} \exp\left(-\frac{x^2 - 2\rho(2,0)xy + y^2}{2(1-\rho(2,0)^2)}\right) . \qquad (55)$$

In an analogous way one arrives at the expression for the activity at the third time step

$$\begin{aligned} a(3) &= \left\langle\!\!\left\langle \int \mathcal{D}w^{2,0}(x,y)\, \mathrm{g}_b^2\Big(\xi^1 m^1(2) + \right.\right. \\ &\qquad \left.\left. \alpha\chi(1)\left[\mathrm{g}_b(\xi^1 m^1(0) + \sqrt{\alpha a(0)}\, x)\right] + \sqrt{\alpha a(2)}\, y\Big)\right\rangle\!\!\right\rangle . \end{aligned} \qquad (56)$$

From these results, in particular the absence of the $\sigma_i(0)$-term in (50) we see that feedback loops over two time steps exist, but the probability to have loops over a longer time period equals zero. If the dilution is asymmetric [2], even all feedback disappears and the local field is simply Gaussian distributed. For the special case of $Q = 2$ these results agree with the results available for the first three time steps in the literature [5]-[6].

A4: Fourth step dynamics

Again, from eqs. (24)-(26) we find

$$h_i(3) = \xi_i^1 m^1(3) + \alpha\chi(2)\sigma_i(2) + \mathcal{N}(0, \alpha a(3))\,. \tag{57}$$

with

$$\begin{aligned}
\chi(2) &= \Bigg\langle\!\!\Bigg\langle \frac{1}{\sqrt{\alpha a(2)(1-\rho(2,0)^2)}} \int \mathcal{D}z\, z \int \mathcal{D}y\, g_b \Big(\xi^1 m(2) \\
&+ \alpha\chi(1) g_b(\xi^1 m(0) + \sqrt{\alpha a(0)}\, y) \\
&+ \sqrt{\alpha a(2)(1-\rho(2,0)^2)}\, z + \sqrt{\alpha a(2)}\, \rho(2,0) y \Big) \Bigg\rangle\!\!\Bigg\rangle\,.
\end{aligned} \tag{58}$$

This leads to the main overlap for the fourth time step

$$m^1(4) = \frac{1}{A} \Big\langle\!\!\Big\langle \xi^1 \mathrm{g}_b \Big(\xi^1 m^1(3) + \alpha\chi(2)\sigma(2) + \sqrt{\alpha a(3)}\, z \Big) \Big\rangle\!\!\Big\rangle \tag{59}$$

with z the Gaussian random variables $\mathcal{N}(0,1)$. The average has to be taken over $\xi^1, z, \sigma_i(0)$, and $\sigma_i(2)$ or recalling the evolution equation (5) over $\xi^1, z, \sigma_i(0)$ and $h_i(1)$. The distribution function of these variables, i.e., $\mathcal{D}w^{3,1}(x,y)$ is given by eq. (55) with the index 2 replaced by 3 and 0 by 1. The correlation coefficients between the fields at different time steps can again be calculated from the recursion relation (25)

$$\begin{aligned}
\rho(3,1) &= \frac{1}{\sqrt{a(1)a(3)}} \Big\langle\!\!\Big\langle \int \mathcal{D}w^{2,0}(x,y)\, \mathrm{g}_b \Big(\xi^1 m^1(0) + \sqrt{\alpha a(0)} x \Big) \\
&\quad \times \mathrm{g}_b \Big(\xi^1 m^1(2) + \alpha\chi(1) \mathrm{g}_b \Big(\xi^1 m^1(0) + \sqrt{\alpha a(0)} x \Big) + \sqrt{\alpha a(2)} y \Big) \Big\rangle\!\!\Big\rangle\,.
\end{aligned} \tag{60}$$

Using all this eq. (59) becomes

$$
\begin{aligned}
m^1(4) \;=\;& \frac{1}{A}\left\langle\!\!\left\langle \xi^1 \int \mathcal{D}w^{3,1}(x,y)\mathrm{g}_b\Big(\xi^1 m^1(3)\right.\right. \\
&+\; \alpha\chi(2)\mathrm{g}_b\Big(\xi^1 m^1(1)+\alpha\chi(0)\sigma(0)+\sqrt{\alpha a(1)}\,x\Big) \\
&+\; \left.\left.\sqrt{\alpha a(3)}\,y\Big)\right\rangle\!\!\right\rangle\,. \qquad (61)
\end{aligned}
$$

In an analogous way the activity at the fourth time step can be calculated

$$
\begin{aligned}
a^1(4) \;=\;& \frac{1}{A}\left\langle\!\!\left\langle \xi^1 \int \mathcal{D}w^{3,1}(x,y)\mathrm{g}_b^2\Big(\xi^1 m^1(3)\right.\right. \\
&+\; \alpha\chi(2)\mathrm{g}_b\Big(\xi^1 m^1(1)+\alpha\chi(0)\sigma(0)+\sqrt{\alpha a(1)}\,x\Big) \\
&+\; \left.\left.\sqrt{\alpha a(3)}\,y\Big)\right\rangle\!\!\right\rangle\,. \qquad (62)
\end{aligned}
$$

Finally we present the calculations for the fifth time step.

A5: Fifth step dynamics

The local field $h_i(4)$ reads

$$h_i(4)=\xi_i^1 m^1(4)+\alpha\chi(3)\sigma_i(3)+\mathcal{N}(0,\alpha a(4))\,. \qquad (63)$$

The expression for $\chi(3)$ has an analogous form as the one for $\chi(2)$ since the structure of $h_i(3)$, needed to calculate it, is similar as the one of $h_i(2)$

$$
\begin{aligned}
\chi(3) \;=\;& \left\langle\!\!\left\langle \frac{1}{\sqrt{\alpha a(3)(1-\rho(3,1)^2)}} \int \mathcal{D}z\,z \int \mathcal{D}y\,g_b\Big(\xi^1 m(3)\right.\right. \\
+\;& \alpha\chi(2)g_b(\xi^1 m(1)+\alpha\chi(0)\sigma(0)+\sqrt{\alpha a(1)}\,y) \\
+\;& \left.\left.\sqrt{\alpha a(3)(1-\rho(3,1)^2)}\,z+\sqrt{\alpha a(3)}\,\rho(3,1)y\;\Big)\right\rangle\!\!\right\rangle\,. \qquad (64)
\end{aligned}
$$

The overlap at time step five is then given by

$$m^1(5)=\frac{1}{A}\left\langle\!\!\left\langle \xi^1\mathrm{g}_b\Big(\xi^1 m^1(4)+\alpha\chi(3)\sigma(3)+\sqrt{\alpha a(4)}\,z\Big)\right\rangle\!\!\right\rangle \qquad (65)$$

with z the Gaussian random variables $\mathcal{N}(0,1)$. The average has to be taken over $\xi^1, z, \sigma_i(0)$, and $\sigma_i(3)$. Rewriting the network configuration $\{\sigma_i(3)\}$ by means of the gain function (5) the local fields at time steps $0,2$ and 4 appear. The distribution function of these three local fields equals

$$\mathcal{D}w^{4,2,0}(x,y,z) = \frac{dx\ dy\ dz}{(2\pi)^{3/2}\sqrt{\mathrm{Det} w^{4,2,0}}} \exp\left(-\frac{1}{2}\begin{pmatrix} x & y & z \end{pmatrix} (w^{4,2,0})^{-1} \begin{pmatrix} x \\ y \\ z \end{pmatrix}\right) \tag{66}$$

where

$$w^{4,2,0} = \begin{pmatrix} 1 & \rho(2,0) & \rho(4,0) \\ \rho(2,0) & 1 & \rho(4,2) \\ \rho(4,0) & \rho(4,2) & 1 \end{pmatrix} \tag{67}$$

with the correlation coefficients $\rho(2,0), \rho(4,0)$ and $\rho(4,2)$.

The correlation coefficients between the fields at different time steps not mentioned before can again be calculated using the relation (25). They read

$$\begin{aligned} \rho(4,0) &= \frac{1}{\sqrt{a(0)a(4)}} \left\langle\!\!\left\langle \sigma(0) \int \mathcal{D}w^{3,1}(x,y) \right.\right. \\ &\quad \times \mathrm{g}_b\left(\xi^1 m^1(3) + \alpha\chi(2)\mathrm{g}_b\left(\xi^1 m^1(1) + \alpha\chi(0)\sigma(0) + \sqrt{\alpha a(1)}\, x\right)\right. \\ &\quad \left.\left.\left. + \sqrt{\alpha a(3)} y\right)\right\rangle\!\!\right\rangle \end{aligned} \tag{68}$$

and

$$\begin{aligned} \rho(4,2) &= \frac{1}{\sqrt{a(2)a(4)}} \left\langle\!\!\left\langle \int \mathcal{D}w^{3,1}(x,y)\, \mathrm{g}_b\left(\xi^1 m^1(1) + \alpha\chi(0)\sigma(0) + \sqrt{\alpha a(1)}\, x\right)\right.\right. \\ &\quad \times \mathrm{g}_b\left(\xi^1 m^1(3) + \alpha\chi(2)\mathrm{g}_b\left(\xi^1 m^1(1) + \alpha\chi(0)\sigma(0) + \sqrt{\alpha a(1)}\, x\right)\right. \\ &\quad \left.\left.\left. + \sqrt{\alpha a(3)}\, y\right)\right\rangle\!\!\right\rangle . \end{aligned} \tag{69}$$

Using all this eq. (65) becomes

$$\begin{aligned} m^1(5) &= \frac{1}{A} \left\langle\!\!\left\langle \xi^1 \int \mathcal{D}w^{4,2,0}(x,y,z) \mathrm{g}_b\left(\xi^1 m^1(4)\right.\right.\right. \\ &\quad + \alpha\chi(3)\mathrm{g}_b\left(\xi^1 m^1(2) + \alpha\chi(1)\mathrm{g}_b\left(\xi^1 m^1(0) + \sqrt{\alpha a(0)}\, x\right) + \sqrt{\alpha a(2)}\, y\right) \\ &\quad \left.\left.\left. + \sqrt{\alpha a(4)}\, z\right)\right\rangle\!\!\right\rangle . \end{aligned} \tag{70}$$

In an analogous way the activity at the fifth time step can be calculated

$$
\begin{aligned}
a^1(5) \;=\; & \frac{1}{A}\left\langle\!\!\left\langle \xi^1 \int \mathcal{D}w^{4,2,0}(x,y,z)\,\mathrm{g}_b^2 \Big(\xi^1 m^1(4) \right.\right. \\
& + \; \alpha\chi(3)\mathrm{g}_b \Big(\xi^1 m^1(2) + \alpha\chi(1)\mathrm{g}_b \Big(\xi^1 m^1(0) + \sqrt{\alpha a(0)}\,x\Big) + \sqrt{\alpha a(2)}\,y\Big) \\
& \left.\left. + \; \sqrt{\alpha a(4)}\,z\Big)\Big)\right\rangle\!\!\right\rangle \, . \qquad (71)
\end{aligned}
$$

Since the numerical results explicitly show that five time steps do give already an accurate picture of the dynamics in the retrieval regime of the network we do not write out further steps.

A6: Remarks on Q=2

We recall that for $Q = 2$ the following simplifications are possible: $b(s_{k+1} + s_k) = 0, (s_{k+1} - s_k) = 2,\ \mathrm{g}_b(\cdot) = \mathrm{sign}(\cdot)$ and $a(t) = A = 1$. Since the first three time steps for this special case are derived in the literature [5]-[6] we give here, as an illustration, the formula for the overlap for $t = 4$

$$
\begin{aligned}
m^1(4) \;=\; & \sum_{\sigma=\pm 1} \frac{1+\sigma m^1(0)}{2} \int \mathcal{D}w^{3,1}(x,y) \\
& \mathrm{sign}\Big(m^1(3) + \alpha\chi(2)\left[\mathrm{sign}(m^1(1) + \sigma\alpha\chi(0) + \sqrt{\alpha}\,x)\right] + \sqrt{\alpha}\,y\Big) \, . \qquad (72)
\end{aligned}
$$

In comparison with the fully connected model we remark that only two correlated Gaussians are present here and the term in $\chi(1)$ is absent. Furthermore, the ansatz used in [7] for the study of neighbouring trajectories amounts to neglecting the correlations between the Gaussian and discrete part of the noise. The result of this approximation is to take all correlation coefficients $\rho(t, t-2) = 0$ (such that, e.g., the matrix $w^{3,1}$ in the formula (72) above becomes the unit matrix).